

Quantifying the Properties of a Dosimeter Responsive to Blue Light Hazard Effective Wavelengths

A dissertation submitted by

Om Shanaf Abudabous

For the award of

Master of Science (Research)

2014

ACKNOWLEDGEMENTS

I would like to express my special thanks of gratitude to my supervisor Professor Alfio Parisi, who gave me the golden opportunity to do this wonderful project on the topic “Quantifying the Properties of a Dosimeter Responsive to Blue Light Hazard Effective Wavelengths”, which also helped me in doing a lot of research and I came to know about so many new things. I am really thankful to my husband and my kids who have supported me a lot to finalize this work within the time. I would also like to thank my family and friends who have always paid attention about what I did in my project, and morally help has also been given. I would like to thank the Physical Sciences staff of the University of Southern Queensland for their support over the course of this program. Finally, I am doing this project not only for marks but to also increase my knowledge.

Certification of Dissertation

I certify that the ideas, experimental work, results, analyses, software and conclusions reported in this dissertation are my own effort, except where otherwise acknowledged. I also certify that work is original and has not been previously submitted for any other award, except where otherwise acknowledged.

Signature of Candidate

Date

ENDORSEMENT

Signature of Supervisor

Date

ABSTRACT

The research reported in this dissertation characterizes the properties of a proposed blue light dosimeter suitable for measuring the ocular blue light hazard. Blue light of high intensity with shorter wavelengths (400-500 nm) has been shown to produce an adverse effect on the healthy human eye, and the hypothesis proposed is that a dosimeter based on polysulphone and phenothiazine has the properties to act as a dosimeter to measure exposure to the blue light hazard. Exposure to the shorter wavelengths of blue light is measured by weighting the spectral irradiance of a light source against the blue light hazard action spectrum, and the dosimeter employed in this study uses a long pass filter to remove ultraviolet wavelengths shorter than 380 nm. An examination of the polysulphone and phenothiazine dosimeters was completed for the change in absorbance, dose response, the dark reaction, repeatability of measurement, the influence of the angle of the receiving plane, and stability against changes in irradiation and temperature. The results show that a change in the dosimeter optical transmission occurs as a result of exposure to blue light, with maximum dosimeter response after exposure to wavelengths around 420 nm. The polysulphone and phenothiazine dosimeters were exposed to four light sources and dose response calibration curves established that relate blue light exposure to the change in absorbance. The effect of the angle of the receiving plane was found to be approximated by a cosine function for angles up to 70° from the normal, with the difference between measured and theoretical values in this angle range being less than about 0.2. Dosimeter response to repeated solar radiation exposure was found to be reproducible with a standard error in the ΔA of 0.005. The dark reaction of the dosimeter

in terms of the average change in absorbance in darkness was also found to be small, with a change of 0.056 at zero hours being 0.058 after 24 hours and 0.067 after one week. Dosimeter rate variations with irradiance variations between 10 W/m² and 15 W/m² were found to be only $\pm 10\%$, and thus within the measurement error of the badges. Dosimeter responses were also found to be stable for temperatures ranging from 23 °C to 37 °C. Taken together, all these results lead to the conclusion that polysulphone and phenothiazine dosimeters have characteristics that enable their widespread use for rapid, convenient and low-cost assessment of the blue light hazard.

Table of Contents

Acknowledgments.....	i
Certification of Dissertation.....	ii
Abstract.....	iii
List of figures.....	vii
List of tables.....	viii
1. CHAPTER ONE	1
1.1 Introduction	1
2. CHAPTER TWO	3
2.1 Literature Review and Scope of the Project	3
2.2 Electromagnetic Radiation and Eye Damage	3
2.2.1 Electromagnetic Radiation	3
2.3 Eye Damage.....	4
2.4 Action Spectrum.....	6
2.5 Blue Light Hazard	8
2.6 Measurement Techniques.....	10
2.7 Research Project	14
2.7.1 Research Hypothesis.....	14
2.7.2 Research Objectives	14
3. CHAPTER THREE	15
3.1 Methodology.....	15
3.1.1 Equipment and Materials:	15
3.1.2 Dosimeters	15
3.2 Blue Light Hazard Exposure.....	16
3.3 Making Dosimeters	17
3.4 Change in Absorbance	18
3.5 Dose response.....	19
3.6 Influence of the Angle of the Receiving Plane	30

3.7	Dose Rate Independence:	31
3.8	Reproducibility	34
3.8.1	Dark reaction.....	34
3.9	Temperature Independence:	35
4.	CHAPTER FOUR	36
4.1	Results.....	36
4.1.1	Change in Absorbance	36
4.1.2	Dose Response	38
4.1.3	Influence of the Angle of the Receiving Plane	42
4.1.4	Dose Rate Independence	43
4.1.5	Dark Reaction.....	44
4.1.6	Temperature Independence	46
5.	CHAPTER FIVE.....	47
5.1	Discussion.....	47
5.1.1	Change in Absorbance	47
5.1.2	Dose Response	47
5.1.3	Influence of the Angle of the Receiving Plane	49
5.1.4	Dose Rate Independence	49
5.1.5	Dark reaction.....	50
5.1.6	Temperature Independence	51
5.2	Significance	52
5.3	Future Directions	52
6.	CHAPTER SIX.....	54
6.1	Conclusion.....	54
7.	REFERENCES	56
8.	LIST OF ABBREVIATIONS	58

LIST OF FIGURES

Figure 1 Blue light hazard action spectrum (ICNIRP, 1997).....	8
Figure 2 Dosimeter with polysulphone and phenothiazine films and a Llumiar filter.....	17
Figure 3 LED light exposure for eight dosimeters to determine the dose response.....	20
Figure 4 The spectral irradiance for the LED light	21
Figure 5 Exposing the dosimeters for the dose response compact fluorescent lamp (15 W, 5000 K).....	22
Figure 6 The spectral irradiance for a compact fluorescent lamp	23
Figure 7 The spectral irradiance for the solar simulator	25
Figure 8 A fluorescent light exposing ten dosimeters at 10 cm	27
Figure 9 The spectral irradiance for the fluorescent light.....	28
Figure 10 A solar simulator exposing dosimeters at different angles.....	30
Figure 11 The fluorescent tube exposing dosimeters at different distances of 5 cm, 10 cm, 15 cm and 20 cm	32
Figure 12 The spectral irradiances of the fluorescent lamp at distances of 5 cm, 10 cm, 15 cm and 20 cm.	33
Figure 13 The pre exposure spectral transmission averaged over ten dosimeters (top curve) and the average post exposure (bottom curve) spectral transmission following exposure to sunlight.	36
Figure 14 The spectral transmission averaged over twenty dosimeters for pre (top curve) and post exposure (bottom curve) to a lamp.....	37
Figure 15 The blue light hazard exposure dose response for the LED source	38
Figure 16 The blue light hazard for the exposure dose response for the compact fluorescent source	39
Figure 17 Dose response for the solar simulator lamp	40
Figure 18 The dose response curve for the fluorescent tube light.	41
Figure 19 The response to a collimated beam incident at a plane inclined for the following angles: 10°, 20°, 30°, 40°, 50°, 60° and 70°.....	42
Figure 20 The change in absorbance at different irradiances at different distances of 5 cm, 10 cm, 15 cm and 20 cm.....	43
Figure 21 The dark reaction of the blue light dosimeters at periods of zero hours, one day and seven days	45
Figure 22 The change in absorbance for temperatures between 20° and 40° with the average for each dosimeter.....	46

LIST OF TABLES

Table 1 Sunlight exposure data collection dates and times.....	18
Table 2 Lamp exposure data collection dates and times	19
Table 3 Exposure periods for the dose response for six dosimeters to the LED light.....	21
Table 4 Exposure periods for the dose response for dosimeters 71-80 from the compact fluorescent lamp.....	24
Table 5 Exposure periods for the dose response from the solar simulator	26
Table 6 Exposure periods for the dose response for the fluorescent light.....	29
Table 7 Different angles with different dosimeters data collection	31
Table 8 The exposure times and irradiances for the dose rate independence.....	33
Table 9 Data collection with different temperatures.....	35
Table 10 Dark reaction (zero hours, one day and seven days)	44

1. CHAPTER ONE

1.1 Introduction

Sunlight, UV exposure and temperature are potential etiological factors that can cause harmful diseases of the human eye especially affecting the retina. Blue light at relatively high intensities with shorter wavelengths (400-500 nm) produces an adverse effect on the healthy human eye. Diseases such as retinal injury (photoretinitis) are caused by either extremely bright light on the eye for a short time or a less bright light on the eye for a longer exposure period (Sliney, 2001). An action spectrum provides the relative efficiency or the relative harmful effect of radiation at different wavelengths for a particular biological influencing effect (Parisi et al., 2004). A better understanding of the blue light environment is necessary in order to improve preventative measures aimed at reducing the risk of eye damage. Previous research has shown that blue light can trigger damage to the eye. The excessive ocular blue light exposure may contribute to age linked macular degeneration (AMD) (Walker et al., 2012). In order to reduce the implications on public health due to the blue light hazard, it is necessary to first quantify the amount of blue light received by humans during normal daily activities. To decrease these problems, a dosimeter is very helpful for quantifying blue light hazard effective exposures.

The discussion that follows will give a general overview of quantifying the properties of a dosimeter responsive to blue light hazard effective wavelengths, followed by effects of blue light hazard that can trigger a reaction in the human retina. A variety of factors to consider in the measurement of the blue light hazard will be discussed followed by a brief

examination of the methods currently used for measuring the blue light hazard. Specific attention is given to the area of dosimetry as it is an effective tool that is used in the measurement of UV radiation exposures, such as polysulphone and phenothiazine. A potential dosimeter for measuring the blue light hazard effective wavelengths has been proposed (Turnbull and Parisi, 2012).

This project will study whether the proposed blue light dosimeter has the properties suitable for measuring ocular blue light hazard exposures, by testing the change in: absorbance, dose response, influence of the angle of the receiving plane, reproducibility, dark reaction, dose rate independence and temperature independence. Finally, this project will contribute to the previous research by characterizing the properties and the associated errors of the dosimeter for quantifying the blue light hazard exposures.

2. CHAPTER TWO

2.1 Literature Review and Scope of Project

2.2 Electromagnetic Radiation and Eye Damage

2.2.1 Electromagnetic Radiation

Electromagnetic radiation presents both wave (oscillatory) and particle (photon) characteristics (Taylor, 1989). The energy transmitted by a photon is inversely related to its frequency; therefore, the shorter the wavelength the greater will be the energy produced. The energy of a photon is absorbed by the atom or molecule with which it collides. Photons with little energy will still carry sufficient energy to affect the rotation of an atom or a molecule and so can create warming. The higher energy UV photons can change the energy state of the electrons to make the atom electronically excited. Both nucleic acid and proteins within the cells can absorb the energy of UV photons (Taylor, 1989).

2.3 Eye Damage

The eye has greater sensitivity to injury by some wavelengths than others (Taylor, 1989). The high-energy radiation in the solar spectrum especially UV in sunlight is harmful to the human eye. It is especially hazardous to the retina (Young, 1994). The health of the eye is impacted on by UV radiation, heat and oxidation. For example, in the United States, nearly 1 in 5 individuals suffer from eye damage caused by UV radiation before the age of 75 years and nearly one-half of the population by the age of 84 (Young, 1994). The effect of UV radiation can be injurious to the lens of the eye, as it can significantly hasten its deterioration and can eventually culminate in visual impairment and blindness (Young, 1994).

In New Zealand it has been found that the number of eye operations decreases with latitude (Young, 1994). Eye operations are also more prevalent in coastal areas subjected to bright sunshine than in inland areas (Young, 1994). The photons with the greatest energy transmitted to the retina are the most dangerous to the eye. For instance, when the photon energy is high (the blue/violet area of the visible spectrum and the UV), the radiation can be harmful to the retina (Young, 1994). At wavelengths of UV radiation between 320 and 400 nm the lens absorbs the radiation strongly. UV is injurious to the lens cells, specifically those in the nucleus that have a very slow rate of repair (Gies & Roy, 1988). Also, UV radiation affects the retina as approximately 1% of the UVA radiation to the eye reaches the retina (Gies & Roy, 1988). Retinal disease (photoretinitis) can be caused by either extremely bright light for a short exposure time or by a less bright light for a longer exposure time (Sloney, 2001). Sunlight and UV exposure and

temperature are potential etiological factors that can produce harmful diseases of the eye such as pterygium and droplet keratopathies (Sliney, 2001). When the cornea and lens absorb higher wavelengths the retina is consequently exposed to visible light including blue light (Fletcher et al., 2008). Blue light injuries can be sustained by both the retinal pigment epithelium and choriocapillaris through generation of responsive oxygen species and may be a factor in the pathogenesis of age related macular degeneration (AMD) (Fletcher et al., 2008). The retina is more exposed to blue light at younger ages due to the transmission of the lens (Fletcher et al., 2008). The Beaver Dam Eye Study demonstrated that leisure time outdoors in the young adult life was correlated with the incidence of early AMD (Fletcher et al., 2008).

The Chesapeake Bay Watermen Study obtained occupational exposure data over the previous 20 years and discovered no association between UVA and UVB light with AMD (Fletcher et al., 2008). However, the study did note an adverse relationship between blue light and eye damage involving atrophy and scarring (Fletcher et al., 2008). Fletcher et al (2008) also discovered that the combination of blue light exposure and low plasma concentrations of antioxidants was also related with the early stages of AMD and also that blue light exposure in middle age could be more harmful than at younger ages.

Additionally, UV radiation between 180-400 nm can cause several diseases of the eye including erythema, carcinogenesis, corneal photokeratitides and lens cataracts (Walker et al., 2012). The human cornea transmits radiant energy only at 295 nm and above (and thus not in the UVC range). Indeed, all UVC (100- 280 nm) radiations are absorbed by the human cornea which absorbs radiation (Sliney, 2012). Also, blue light triggers retinal injury (photoretinitis) and is implicated in the pathogenesis of AMD (Walker et al.,

2012). Several researchers have reported that the retinal-pigmented epithelium (RPE), a cellular layer of the retina responsible for its nourishment, is also injured or destroyed by excessive blue light exposure (Walker et al., 2012). Each blue light exposure contributes to the cumulative creation of cytotoxic photoproducts. Individuals who are chronically exposed to blue light will be at greater risk of contracting AMD (Walker et al., 2012). Moreover, lipofuscin (cellular debris) accumulates in the retinal pigments epithelium (RPE) (Roberts, 2011). Blue light waves could be especially toxic to those who are prone to macular problems due to several factors including genetics, nutrition, environment, health habits and ageing (Roberts, 2011).

When a photon hits a photoreceptor cell in the retina, it should not be responsive to light until it has recovered from the blue light waves. It has been shown in rodents that absorption of blue light can cause the photoreceptor to detect light before it is ready (Roberts, 2011). This significantly raises the potential for oxidative injury, which leads to a build-up of lipofuscin in the (RPE) layer (Roberts, 2011). Finally, if there are high quantities of blue light absorbed by lipofuscin, it can become phototoxic leading to oxidative injury to the RPE and more cell death (Roberts, 2011). Therefore, the blue light can cause several diseases to the eye that can affect the retina, RPE and AMD.

2.4 Action Spectrum

The relative effectiveness of different wavelengths for producing a particular biologic effect is given by a function called the action spectrum (equation 1) (Oliva & Taylor,

2005). Each action spectrum is generally normalized at the wavelength with the highest response, which is given a unity value. For a particular action spectrum with a biologically effective irradiance E_{BE} , an action spectrum provides the relative effectiveness or relative damaging effect of UV for a particular biological process (Parisi et al., 2004):

$$E_{BE} = \int_{\lambda} S(\lambda)A(\lambda)d\lambda \quad (\text{Equation 1})$$

Where $A(\lambda)$ is the action spectrum, $S(\lambda)$ is the spectral irradiance in $\text{Wm}^{-2} \text{nm}^{-1}$ and λ is the wavelength increment.

The action spectrum for erythema in humans has been used commonly for measuring the UV effect on human skin. The weighting of this action spectrum is normalized to unity 298 nm and shorter wavelengths and the biological effectiveness decreases by approximately a factor of 1000 at 320 nm (CIE, 1987).

The meaning of the action spectrum is the amount of irradiation at a given wavelength or band of wavelengths that can lead to damage (Taylor, 1989). It is the threshold for a specific effect and is particular to specific tissues (Taylor, 1989). The action spectrum for the human cornea is mostly related to that of subhuman primates, while the human cornea is more sensitive to UV radiation than is the cornea of animals (Taylor, 1989). To determine an action spectrum scientists employ various methods to detect changes in the retina for specific wavelengths (van Norren & Gorgels, 2011). Biologically effective irradiances are measured in milliWatt per square centimetre (mW cm^{-2}). The exposures of UV radiation given by irradiance over a time period have a radiant exposure given in Joule per square centimetre (J cm^{-2}) (van Norren & Gorgels 2011).

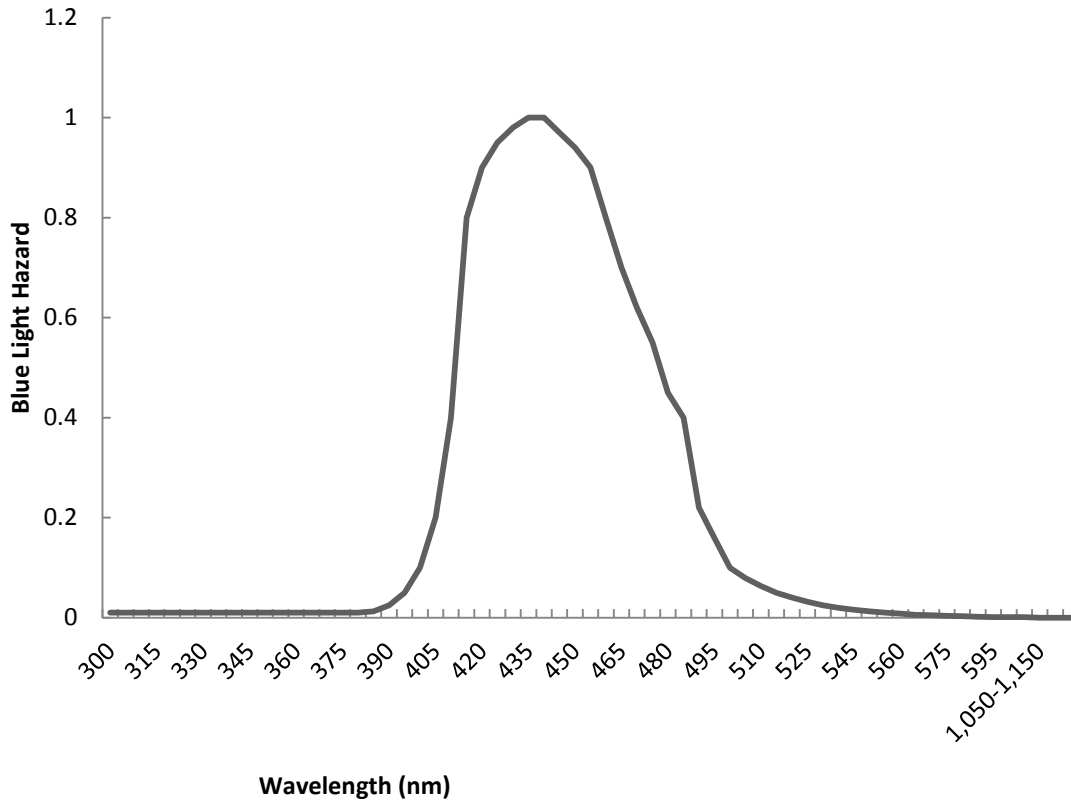


Figure 1 Blue light hazard action spectrum (ICNIRP, 1997)

2.5 Blue Light Hazard

Photochemical retinal injury, known as photoretininitis, is triggered by light mainly in the wavelength region of 400-500 nm. The light in this region appears blue to the eye and so is called blue light (Okuno et al., 2010). The shorter wavelengths pose the greatest hazard because they inversely contain more energy. Exposure to these wavelengths has been called the blue light hazard because these wavelengths appear blue to the human eye and are hazardous (Smith et al., 2005). Blue light is found to cause a reaction in the eye and

has been characterized by the International Commission on Non- Ionising Radiation Protection (ICNIRP) as the blue light hazard (Figure 1). The Y- axis has no units as it is displaying normalized values. Exposure to blue light has been found to affect photoreceptor and retinal pigment epithelium cell function, as well as inducing both photochemical harm and cell death. This blue light photochemical injury to the human retina is termed photoreinitis. The blue light hazard action spectrum is appropriate for broad- band non-laser light sources (ICNIRP, 1997). The hazard of blue light is usually measured by the effective blue light radiance, which is found by weighting the spectral radiance of the light against the blue light hazard action spectrum and integrating this in the wavelength range between 305-700 nm (Okuno et al., 2010). The crystalline lens of the young and healthy human eye has a high level of transparency for optic radiation of short wavelengths ranging between 400-500 nm (SCENIHR, 2012). Also, the blue light hazard action spectrum has been weighted with a sample global solar spectrum. This shows the minor consequences that solar radiation wavelengths below 380 nm and above 560 nm have as compared to the blue light hazard (Turnbull & Parisi, 2012).

Geometrical factors are important in selective sunlight exposure to specific parts of the eye such as the lens, cornea and retina. Many studies have shown that sunlight exposure to local areas of the cornea, lens and retina varies greatly in different environments (Sliney, 2001). Due to the varying amounts of radiation in different environments, it is necessary to have a way to measure these different levels. Dosimetry provides a means to measure such levels.

2.6 Measurement Techniques

The science of the dosimeter is based on knowledge of radiation measurement. There are many reasons for measuring UV and visible radiation. Firstly, measurement of this radiation is necessary to provide safe radiation exposure of patients, animals, cells and plants. Secondly, measurement of radiation is also necessary to enable the effects of irradiations provided in diverse laboratory situations to be published and compared (Diffey, 2002).

The radiometer is a broad-band instrument that is used as a monitor to provide reference measurements, irradiance measurements and exposure measurements over specific wavebands (Diffey, 2002). The UVB detector by International Light (IL) responds to wavelengths of approximately 290-310 nm (Roy et al., 1995). The International Light meter can respond to UVB radiation; however, it also has a smaller response to UVA radiation (Roy et al., 1995). For example, in Melbourne the Solar Light UV biometers (model 501B) have been installed and are also located in the other main Australian capitals (Roy et al., 1995). The IL actinic detectors and the Solar Light UV biometers have important spectral responses related to the erythral action spectrum (Roy et al., 1995). A miniature version of the Sunburn Ultraviolet Meter is a solid-state device that measures 35 mm in diameter by 13 mm in height and uses a magnesium tungsten phosphor. It emits visible light when exposed to UV (Rosenthal et al., 1985). This visible light is converted by a photoelectric diode to an electrical current, which is integrated by the instrument and can then be related to radiant dose (Rosenthal et al., 1985).

Spectroradiometry is the technique for measuring the spectral power distribution in narrow waveband increments (Diffey, 2002). Spectroradiometers have a significant role in measuring radiation for the evaluation of biological hazards (Wengraitis et al., 1998). These instruments can measure the spectral irradiance at every wavelength for their sensitivity range (Wengraitis et al., 1998). Diffusers or integrating spheres are used as the input optics for measurement of spectral irradiance, particularly for extended sources such as linear arrays of fluorescent lamps or day-light. This is to avoid direct irradiation of the entrance slit (Diffey, 2002). Monochromators particularly double monochromators are used mainly because of better stray radiation rejection characteristics (Diffey, 2002). The gratings of the monochromator are moved with a stepper motor to allow scanning of the spectrum.

There are two significant spectroradiometer devices: the Brewer spectroradiometer and the Bentham spectroradiometer. The Brewer MKIII and the Bentham DTM300 are types of monochromator UV spectroradiometers that can be used to measure both the global and the direct solar spectral irradiance and from data analysis the aerosol optical depth (Kazadzis et al., 2005). The Brewer spectroradiometer is a double monochromator instrument involving two identical holographic gratings (3600 lines/mm) (Kazadzis et al., 2005). The instrument has a wavelength range of 287.5 - 366.0 nm. It also has the necessary properties to measure the direct sun spectral irradiances (Kazadzis et al., 2005). The Bentham DTM300 contains a double monochromator with a 300 mm focal length and there are two sets of holographic gratings. The spectral resolution is approximately 0.48 nm (Kazadzis et al., 2005). The Bentham spectroradiometers can be set up to measure the direct sun, diffuse and global spectral irradiances (Kazadzis et al., 2005).

Another type of spectroradiometer is based on a CCD array. A CCD array has been used instead of the holographic gratings and shown to be very constant without variations in sensitivity (at 25° C) in 10 years of operation (Forgan & McGlynn, 2010). The characteristics of CCDs have to be determined before effective measurements can be attempted (Forgan & McGlynn, 2010). The technology of CCD arrays can be used to respond to the ageing of both Dobson spectrophotometers for monitoring ozone and improving a more compact device for monitoring solar UV (Forgan & McGlynn, 2010).

Chemical dosimeters in the ultraviolet waveband can be employed to measure erythemal UV exposures using polysulphone dosimeters (Davis et al., 1976). These polysulphone dosimeters have the necessary properties to be used extensively in research to measure the erythemal UV exposure (Davis et al., 1976). The potential of the photochemical polysulphone (PS) with Naladixic acid (NDA) has been considered as a dosimeter and has been found to have a reaction that extends into the UVA (Davis et al., 1976). Polysulphone is used as a 40-micron polymer film that undergoes photodegradation in the presence of UV resulting in an increase in optical absorbance over a range of wavelengths shorter than 330 nm. Sheets of the polymer film are cut into 2.0 by 2.0 cm squares and mounted on cardboard badges with windows measuring approximately 15 mm in diameter (Rosenthal et al., 1985). Forty micron polysulphone films have been used as a UV dosimeter to measure UVB exposure at seven anatomical sites of volunteers undertaking recreational events (Roy et al., 1995). This film has an advantage in its ease of preparation for use for both analysis and calibration (Roy et al., 1995). The film used in dosimeters of approximately 3 cm x 3 cm has been employed to monitor personal UV exposures during normal daily activities (Diffey, 1984).

There are different types of photoactive chemical dosimeters that have been developed for use in the measurement of UV radiation exposures including polyphenylene oxide, phenothiazine, 8-methoxypsoralen and nalidixic acid (Turnbull & Parisi, 2012). Polysulphone has been shown to have a spectral sensitivity that is high in the UVB region; however, its response above approximately 340 nm is negligible, whereas phenothiazine has been shown to respond to both UVB and UVA wavelengths (Jia et al., 2010). Polysulphone does not react to the blue light but the phenothiazine does react to the blue light. The optical absorbance changes as a result of exposure as measured with a spectrophotometer.

The polysulphone and phenothiazine solution is cast into thin film form of 40 μm thickness. The polysulphone acts like a polymer substrate to prevent the film from being brittle and useable as a thin film. The solution is cast on a glass slab that is optically flat to 1 micron (Turnbull & Parisi, 2012). The technique used for calibration of the dosimeter for the measurement of UVA is to expose a series of dosimeters to different periods of solar UV exposure on a horizontal plane while concurrently measuring the UVA exposure with a calibrated meter (Jia et al., 2010).

These polysulphone and phenothiazine dosimeters are very sensitive to both UVA and UVB and blue light wavebands. In order to create a dosimeter that responds to blue light hazard wavelengths only, a film of the filter Llumiar is used to remove the UVA and UVB wavelengths. The polysulphone and phenothiazine dosimeters alter in optical absorbance (ΔA) as a result of exposure to blue light radiation. The maximum ΔA occurs at 437 nm (Turnbull & Parisi, 2012). This previous research has not characterised the properties of the dosimeter to determine if they are suitable for a blue light hazard dosimeter. The

previous research will be extended to quantify the properties for use as a blue light hazard dosimeter.

2.7 Research Project

2.7.1 *Research Hypothesis*

The hypothesis of this research is that a dosimeter based on polysulphone and phenothiazine has the necessary properties to measure the blue light hazard exposure.

2.7.2 *Research Objectives*

The purpose of this research is to investigate whether a proposed blue light dosimeter has the characteristics suitable for measuring blue light hazard exposures.

The objectives of the research are:

- To evaluate the combined polysulphone and phenothiazine dosimeters for measuring the blue light hazard exposure.
- To characterize the properties of polysulphone and phenothiazine dosimeters. The properties being measured are change in absorbance, dose response, influence of the angle of the receiving plane, dark reaction, reproducibility, dose rate independence and temperature independence.

3. CHAPTER THREE

3.1 Methodology

3.1.1 Equipment and Materials:

- Spectrophotometer: model UV1604, Shimadzu & Co, Kyoto, Japan.
- Spectroradiometer: model DMc150, Bentham instruments, Ltd., Reading, UK.
That has been previously calibrated to a 150 W lamp with calibration traceable to the National Physical Laboratory, UK.
- Light sources: Sunlight, Fluorescent lamps for lighting, Compact Fluorescent lamp (15 W, 5000 K), LED light and Solar simulator Solar simulator (model 15S solar UV simulator, Solar Light Co., Philadelphia, USA).
- Materials for fabricating dosimeters: Phenothiazine, Polysulphone & Llumar.

3.1.2 Dosimeters

Chemical dosimeters are an effective and less costly means of quantifying an individual's level of non-ionizing radiation exposure than electronic dosimeters. Numerous photoactive chemical dosimeters have been developed for use in the measurement of UV radiation exposures such as, polysulphone, phenothiazine, polyphenylene oxide, 8-methoxypsoralen and nalidixic acid (Turnbull & Parisi, 2012). Additionally, these

authors fabricated dosimeters from 40 μm thick film that has phenothiazine as the chromophore. Phenothiazine cannot be cast into a thin film on its own, as it is brittle and not usable as a thin film. Consequently it was mixed with either polysulphone or poly vinyl chloride to allow casting in thin film form (Turnbull and Parisi, 2012). The thin film was cut into pieces of approximately 20 mm x 20 mm and taped onto holders that are 30 mm x 30 mm in size and have a hole of 12 mm x 16 mm over which the thin film is taped. Phenothiazine also responds to the UVA and UVB wavelengths (Parisi et al., 2005). The majority of the irradiances at these wavelengths are removed with the use of Llumar film (Supplier, MEP Films) that is taped over the dosimeters.

3.2 Blue Light Hazard Exposure

To determine the dose response a series of dosimeters will be exposed on a horizontal plane to light from each of sunlight, a fluorescent tube, a compact fluorescent light and a LED light. The spectral irradiance at the plane of the dosimeters will be measured with an UV/visible spectroradiometer (model DMc150, Bentham instruments, Ltd., Reading, UK). This will be done at set intervals to allow for any variation. The blue light hazard effective exposures BL will be calculated (equation 2) for each of the light sources by multiplying the spectral irradiances with the action spectrum (ICNIRP, 1997) as follows:

$$BL = T \sum_{300}^{600} S(\lambda)A(\lambda)\Delta\lambda \quad (\text{Equation 2})$$

where T is the time period in seconds, S (λ) is the spectrum; A (λ) is the action spectrum and $\Delta\lambda$ is the wavelength increment. For each time period a dosimeter will be removed at

set exposures. The ΔA will be measured at four sites over each dosimeter, calculating the average of the four measurements and the standard deviation. For this research the dosimeters will be measured 24 hours post-exposure to take into account the effect of the dark reaction (Turnbull & Parisi, 2012). A calibration curve for each light source will then be calculated. This calibration curve is necessary to determine the blue light hazard exposure for a given change in absorbance.

3.3 Making Dosimeters

The first step of the methodology involved making dosimeters from different films that included polysulphone, phenothiazine and Llumar films. Firstly, the polysulphone was mixed with the phenothiazine in chloroform and cast in thin film. This film was then cut into pieces of approximately 2 cm \times 2 cm. This film was attached with tape over a holder with an opening of 1.2 cm \times 1.6 cm as shown in Figure 2. Llumar was taped over the polysulphone and phenothiazine films to act as a filter in order to block the UV wavelengths.



Figure 2 Dosimeter with polysulphone and phenothiazine films and a Llumar filter

3.4 Change in Absorbance

This experiment investigated the determination of the wavelength at which the maximum change in absorbance (ΔA) occurs due to blue light exposure. Firstly, a batch of 10 dosimeters was measured for their pre exposure transmission from 300 nm to 600 nm in 1 nm increments in a spectrophotometer (model UV1604, Shimadzu Co, Kyoto, Japan). These dosimeters were then exposed on a horizontal plane to 3 hours of sunshine in order to provide a change in the dosimeter. The details of the exposure period are given in Table 1. The dosimeters were then measured for their post exposure transmission from 300 nm to 600 nm. Finally, all the data were collected and analysed to determine the wavelength with the maximum change in absorbance.

Table 1 Sunlight exposure data collection dates and times

Dosimeter Number	Date	Start Time	Stop Time	Cloud Conditions
1-10	18/11/2012	10.24 am	1.24 pm	Nil

Another 10 dosimeters were measured for their pre-exposure transmission from 300 nm to 600 nm. They were then exposed to 5 days of light at 10 cm from a compact fluorescent lamp (15 W, 5000 K) as shown in Table 2 in order to investigate the influence of a different spectrum. Subsequently, these dosimeters were also measured for their post exposure transmission from 300 nm to 600 nm in a spectrophotometer. Thus, for each light source, the average pre exposure transmission and post exposure transmission was plotted to determine the wavelengths where the

maximum change occurred. The analysis found that the maximum change in absorbance ($\lambda_{\Delta\alpha_{max}}$) that occurred was approximately at 420 nm.

Table 2 Lamp exposure data collection dates and times

Dosimeter Number	Start Day	Start Time	Stop Day	Stop Time
11-20	Tuesday	12.30 pm	Sunday	12.30 pm

3.5 Dose response

From the previous section, the wavelength at which the maximum change in absorbance occurred was 420 nm. The spectrophotometer was now set to work in photometric mode at $\lambda_{\Delta\alpha_{max}}$ with the dosimeter holder in place and auto zeroed for each series of measurements. Thirty eight dosimeters were measured for their pre-exposure absorbance at $\lambda_{\Delta\alpha_{max}}$ at four sites over each dosimeter. To determine the dose response, the dosimeters in these series were exposed on a horizontal plane to a solar simulator, and at 10 cm from the fluorescent tube, the compact fluorescent light and the LED light. The setup for the LED light is shown in Figure 3. The spectral irradiance at the plane of the dosimeters from each of the lamp sources was measured with the UV/visible spectroradiometer (model DMc150, Bentham instruments, Ltd, Reading, UK) from 300 nm to 600 nm. Figures 4, 6, 7 and 9 show the spectral irradiances for the four light sources.

Six dosimeters were exposed for up to 6 days of light from the LED light at 10 cm for exposure periods of 46, 54, 69, 77, 92 and 100 hours (Table 3). These dosimeters were measured for their post exposure absorbance at $\lambda_{\Delta_{max}}$. Thus, for each of the exposure intervals, the blue light hazard effective exposure was calculated and a calibration curve was plotted of the exposure versus the resulting change in absorbance.



Figure 3 LED light exposure for eight dosimeters to determine the dose response

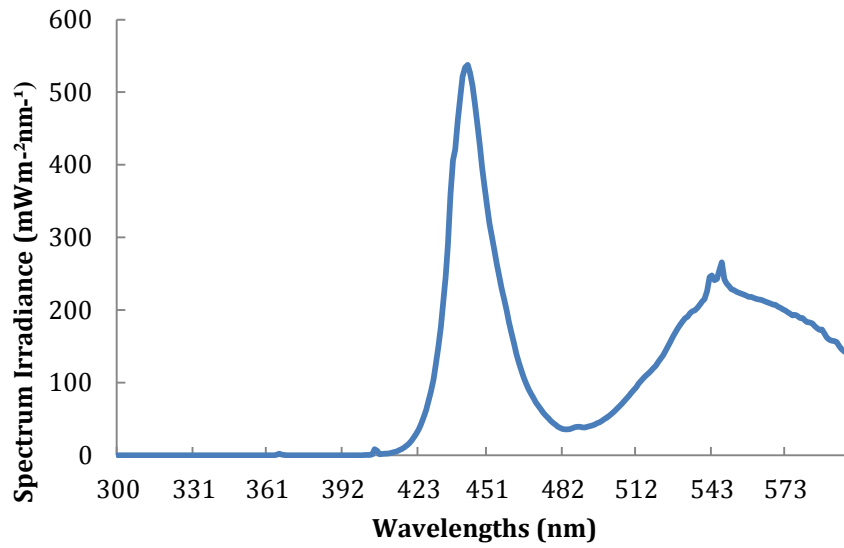


Figure 4 the spectral irradiance for the LED light

Table 3 Exposure periods for the dose response for six dosimeters to the LED light

Dosimeter Number	Start Day	Start Time	Exposure Time (hours)
42	10/08/2013	1.00 pm	46 h
41	11/08/2013	11.00 pm	54 h
40	12/08/2013	2.00 pm	69 h
39	13/08/2013	1.00 pm	77 h
38	14/08/2013	4.00 am	92 h
37	15/08/2013	12.30 pm	100 h

The second type of source light investigated for a dose response was a compact fluorescent light. Ten dosimeters were measured for their pre exposure absorbance at 420 nm at four sites (Table 4). These dosimeters were then exposed to 10 days of light at 10 cm from a compact fluorescent lamp (15 W, 5000 K). Each dosimeter was exposed to the light throughout the day with the exposure times given in Table 4 and then the post-exposure absorbance was measured at 420 nm. This data were analysed to provide the dose response.



Figure 5 Exposing the dosimeters for the dose response compact fluorescent lamp (15 W, 5000 K)

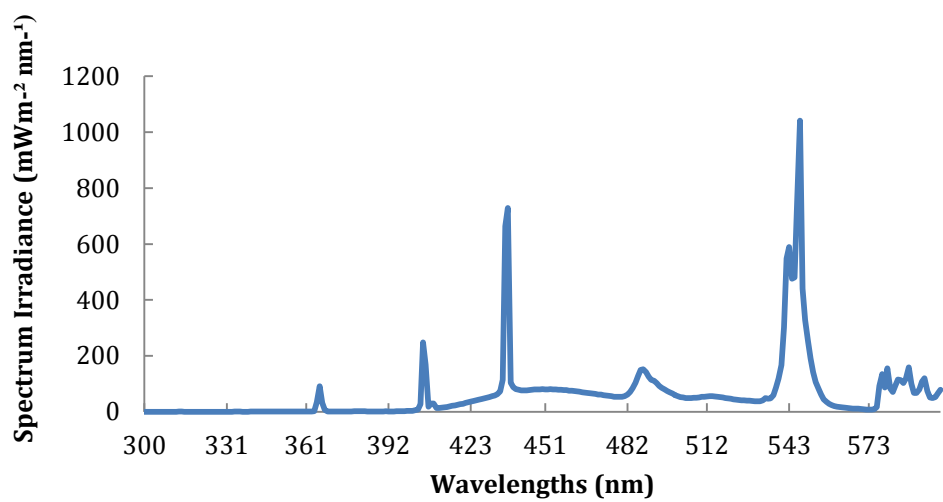


Figure 6 The spectral irradiance for a compact fluorescent lamp

Table 4 Exposure periods for the dose response for dosimeters 71-80 from the compact fluorescent lamp

No. Dosimeters	Date	Exposure Time (hours)
71	14/02/2013	24
72	15/02/2013	48
73	16/02/2013	72
74	17/02/2013	96
75	18/02/2013	120
76	19/02/2013	144
77	20/02/2013	168
78	21/02/2013	192
79	22/02/2013	216
80	23/02/2013	240

The third type of light source was a solar simulator (model 15S solar UV simulator, Solar Light Co., PA, USA). Due to the cloudy weather, this equivalent source to sunlight was used to expose the dosimeters. One dosimeter was measured for the pre-exposure absorbance at 420 nm at four dosimeter sites. Only one dosimeter was exposed due to the small size of the solar simulator beam. This dosimeter was then exposed to the solar simulator at 10 cm. This dosimeter was exposed on a plane normal to the incident radiation (0°). For eight times, at each half hour interval

the dosimeter was measured for the post exposure absorbance (Table 5). All the data were then collected to calculate the average and the difference between the pre and post exposure absorbance. A calibration curve for this light source was then determined.

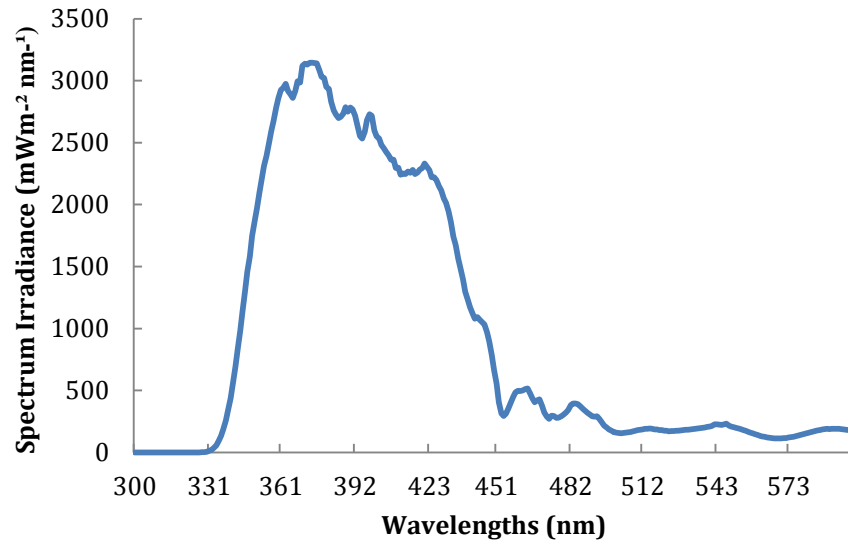


Figure 7 The spectral irradiance for the solar simulator

Table 5 Exposure periods for the dose response from the solar simulator

Start Time	12:45 pm	1:17 pm	1:46 pm	2:17 pm	2:48 pm	3:31 pm	4:01 pm	4:31 pm
Stop Time	1:15 pm	1:45 pm	2:16 pm	2:47 pm	3:30 pm	4:00 pm	4:30 pm	5:00 pm
Exposure Time (hours)	0.5h	0.5 h	0.5 h	0.5 h	0.5 h	0.5 h	0.5 h	0.5 h

The last light source for the dose response was a fluorescent tube (40 Watt). In this part, ten dosimeters were measured for their pre-exposure absorbance and they were exposed for a range of times to the fluorescent tube at 10 cm during ten days (Table 6). Each day, just one dosimeter was taken so the dosimeters were exposed for a range of times from one to ten days. After ten days, all dosimeters were measured for the post exposure absorbance. After all the measurements, the averages and the change in absorbance were calculated to determine a calibration curve.



Figure 8 A fluorescent light exposing ten dosimeters at 10 cm

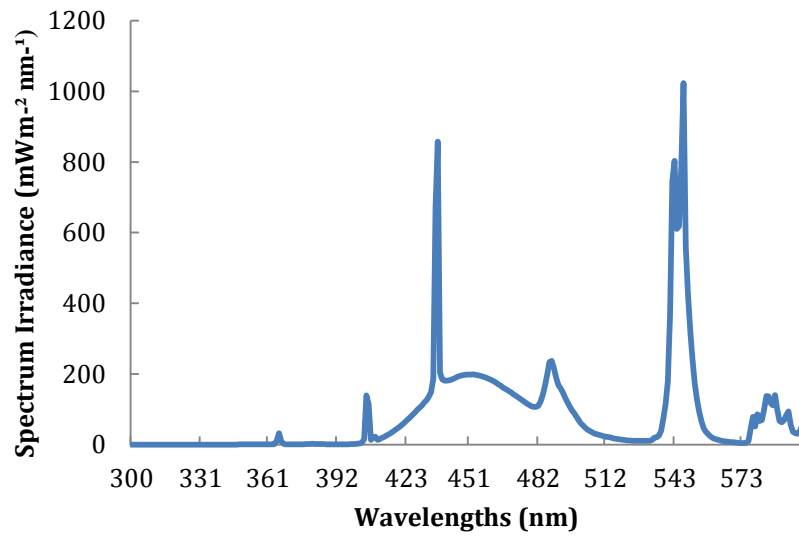


Figure 9 The spectral irradiance for the fluorescent light

Table 6 Exposure periods for the dose response for the fluorescent light

Dosimeter Number	Date	Exposure Time (hours)
91	2/08/2013	24
92	3/08/2013	48
93	4/08/2013	72
94	5/08/2013	96
95	6/08/2013	120
96	7/08/2013	144
97	8/08/2013	168
98	9/08/2013	192
99	10/08/2013	216
100	11/08/2013	240

3.6 Influence of the Angle of the Receiving Plane

The exposures in the previous section with the solar simulator were repeated for planes inclined to the beam. Firstly, seven dosimeters were measured for their pre exposure absorbance at 420 nm. By using a solar simulator being a controlled source, all dosimeters were exposed to the same amount of radiation during two hours at 10 cm at a range of angles normal to the incident irradiance. These different angles were 10° , 20° , 30° , 40° , 50° , 60° and 70° . All dosimeters were then measured for the post exposure absorbance. Thus, the change in absorbance of these dosimeters at a given angle was normalized to 0° incidence.



Figure 10 A solar simulator exposing dosimeters at different angles

Table 7 Different angles with different dosimeters data collection

Dosimeter Number	Angles	Start time	Stop time
82	10°	9:30 am	11:30 am
83	20°	11:30 am	1:30 pm
84	30°	1:30 pm	3:30 pm
85	40°	3:30 pm	5:30 pm
86	50°	11:00 am	1:00 pm
87	60°	1:00 pm	3:00 pm
88	70°	3:00 pm	5:00 pm

3.7 Dose Rate Independence

This experiment was conducted to test the dose rate independence. Firstly, approximately seventeen dosimeters were measured for their pre exposure absorbance in a spectrophotometer at four sites over each dosimeter. These dosimeters were placed at four different distances of 5 cm, 10 cm, 15 cm and 20 cm from a light source. The light source was the fluorescent lamp. All the dosimeters at different distances were exposed for different times (Table 8), so they received the same exposure. The spectral irradiance at each distance was measured with the spectroradiometer and is shown in Figure 12. These irradiances were used to determine the exposure time to produce the same exposure. The dosimeters were then measured for their post exposure

absorbance and all the data were analysed to calculate the average and standard deviation of the ΔA and the dose rate independence.



Figure 11 The fluorescent tube exposing dosimeters at different distances of 5 cm, 10 cm, 15 cm and 20 cm

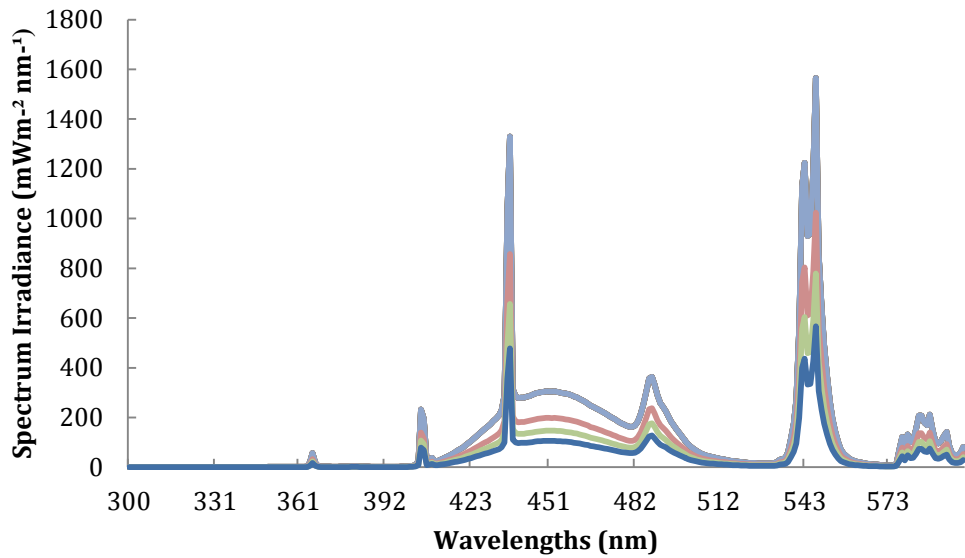


Figure 12 The spectral irradiances of the fluorescent lamp at distances of 5 cm, 10 cm, 15 cm and 20 cm.

Table 8 The exposure times and irradiances for the dose rate independence

Distances (cm)	Exposure Time (hours)	Irradiances (W/m^2)
5	31.1	14.13
10	48	9.17
15	64.7	6.80
20	89.4	4.92

3.8 Reproducibility

This section of the research investigated the reproducibility of the dosimeter. Fifteen dosimeters were exposed on a horizontal plane to an artificial light source for an exposure that produces a measurable ΔA . Firstly, fifteen dosimeters were measured for their pre exposure absorbance at $\lambda_{\Delta a_{max}}$ at four sites over each dosimeter in the spectrophotometer. They were then exposed to the sunlight for four hours. The dosimeters were then measured for the post exposure absorbance at $\lambda_{\Delta a_{max}}$. All data were analysed to find the average and standard error in order to determine the reproducibility.

3.8.1 Dark reaction

Fifteen dosimeters were kept from the previous section in a bag in a cupboard for 24 hours of darkness. These dosimeters were then measured for the post exposure absorbance in a spectrophotometer at four sites over each dosimeter. Data were collected to find the average for the pre and the post exposure. Following this, the fifteen dosimeters were kept in a dark place for seven days and again measured for the post exposure absorbance. All these results were analysed: (0 hours, 24 hours and 7 days) to determine the dark reaction. All these measurements were analysed to determine the dark reaction that occurs post exposure.

3.9 Temperature Independence:

Fifteen dosimeters were measured for their pre exposure absorbance prior to exposure at temperatures between 20^o and 40^o C. Five dosimeters were exposed on a horizontal plane to the fluorescent lamp at 10 cm at each of three temperatures. Three groups of the dosimeters had their temperature measured with a thermometer. The different temperatures were obtained with a hair dryer blowing hot air over the dosimeters. Firstly, before starting this experiment, the temperature was measured after half an hour for each of the three thermometers. The group of dosimeters was exposed to the light source with measurements of the temperature taken at different times (Table 9). Finally, the fifteen dosimeters were measured for the post exposure absorbance at four sites for each dosimeter. The average and standard deviation were calculated to find the effect of temperature.

Table 9 Data collection with different temperatures

Time	Temperature 1	Temperature 2	Temperature 3
0.5 h	22 ^o	25 ^o	35 ^o
3 h	23 ^o	26 ^o	36 ^o
1 day	23.5 ^o	28 ^o	38 ^o
2 days	24 ^o	29 ^o	39 ^o

4. CHAPTER FOUR

4.1 Results

4.1.1 Change in Absorbance

The pre exposure spectral transmission averaged over ten dosimeters and the average post exposure spectral transmission after exposure to sunlight are shown in Figure 13. The maximum change in absorbance between the pre and post exposure values occurs at approximately 420 nm

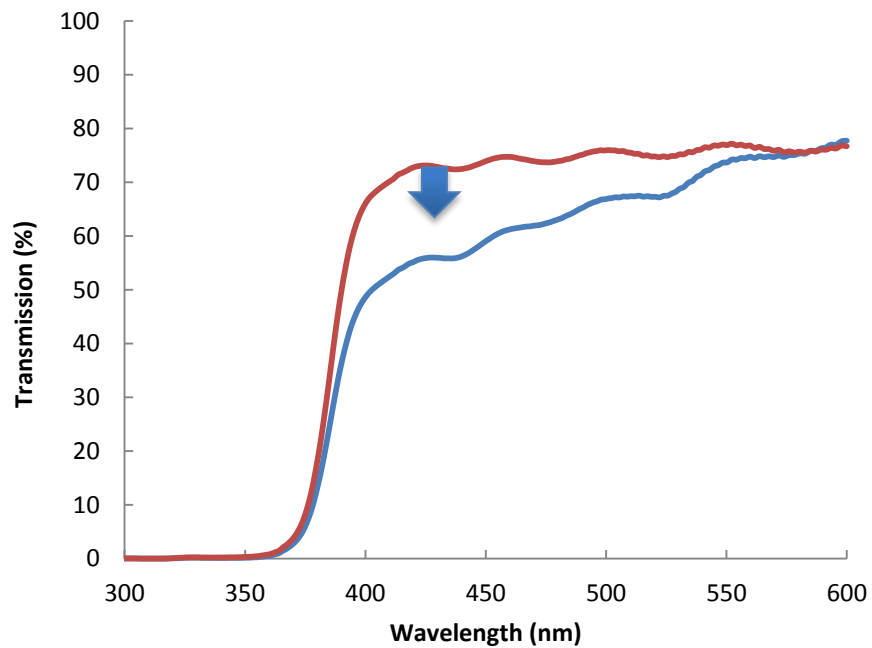


Figure 13 The pre exposure spectral transmission averaged over ten dosimeters (top curve) and the average post exposure (bottom curve) spectral transmission following exposure to sunlight.

Figure 14 shows the pre-exposure spectral transmission averaged for ten dosimeters and the average post exposure transmission after exposure to a compact fluorescent lamp. The maximum change is at approximately 420 nm.

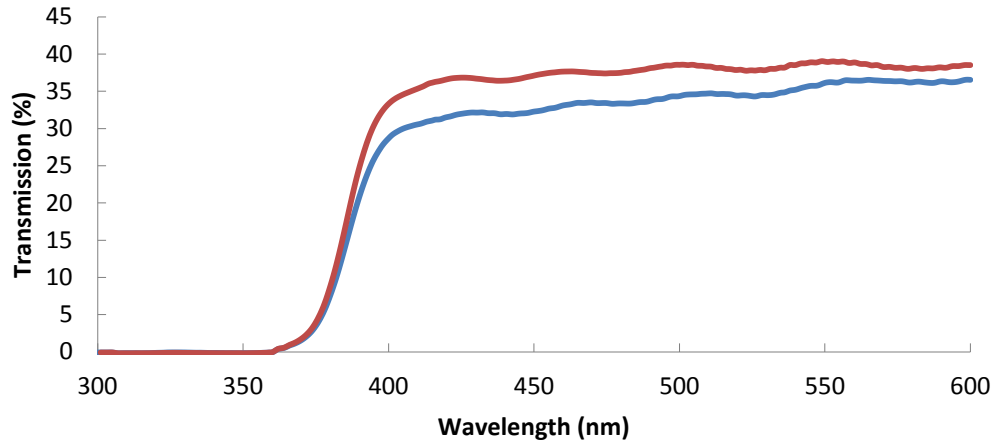


Figure 14 The spectral transmission averaged over twenty dosimeters for pre (top curve) and post exposure (bottom curve) to a lamp

4.1.2 Dose Response

Figure 15 shows the calibration curve for the LED source. The relationship between the blue light exposure and the change in absorbance provides the dose response.

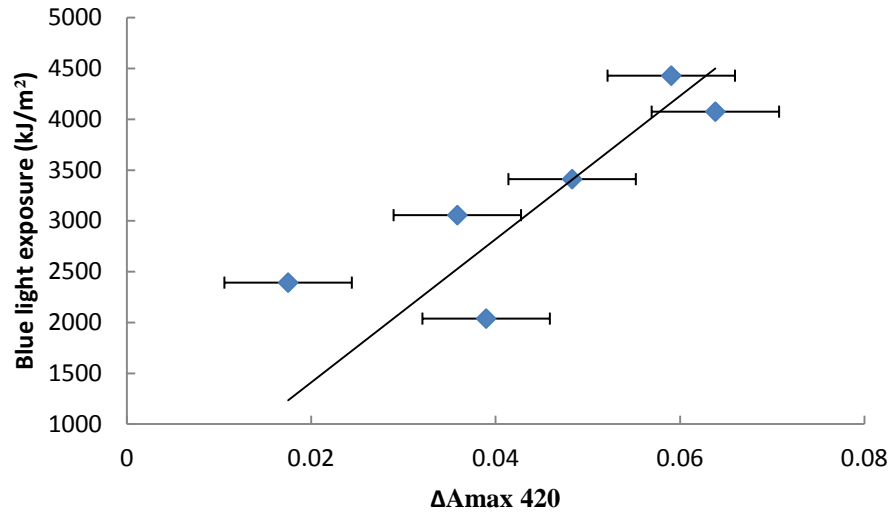


Figure 15 The blue light hazard exposure dose response for the LED source

Figure 16 shows the calibrations curve for a compact fluorescent light source for several days. The dosimeters were calibrated by comparing the change in optical absorbance of the dosimeter with exposures to measure the dose response. All data from the spectral measurements were acquired with the scanning spectroradiometer.

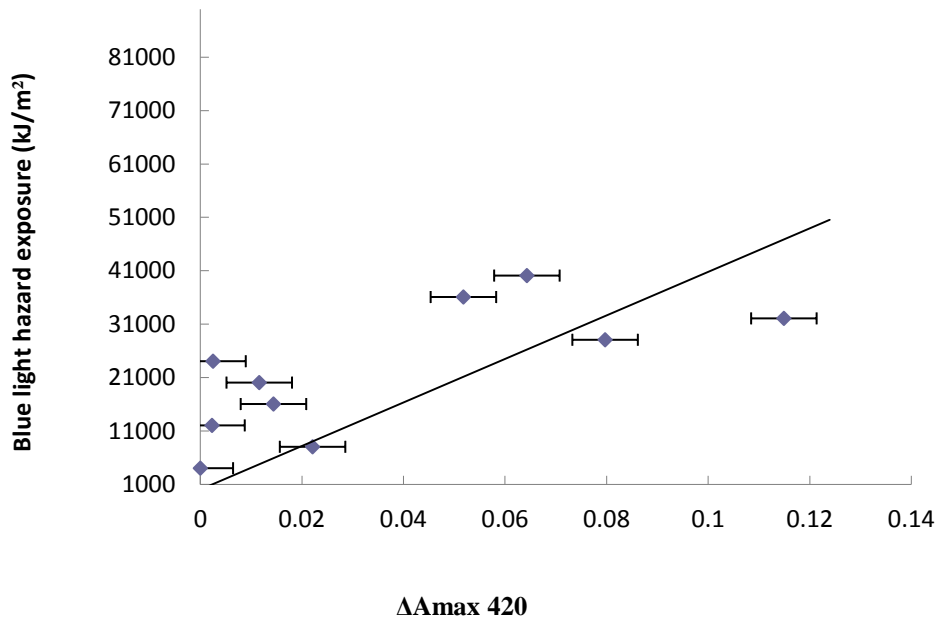


Figure 16 The blue light hazard for the exposure dose response for the compact fluorescent source

Figure 17 shows the relationship between the blue light hazard exposure and the $\Delta A_{MAX} 420$ for the solar simulator. The data positions are the averages of the measured changes in absorbency measured at ($\Delta A_{max} 420$ nm) transversely at four points on each dosimeter. The error bars illustrate the standard deviation of the four measurements.

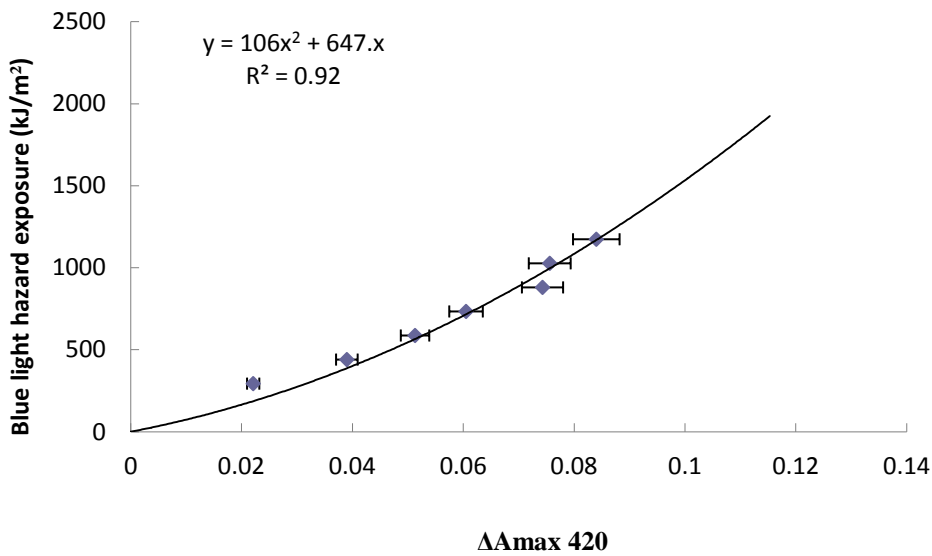


Figure 17 Dose response for the solar simulator lamp

Figure 18 shows the calibration curve for the fluorescent tube. The error bars show the standard deviation for each point.

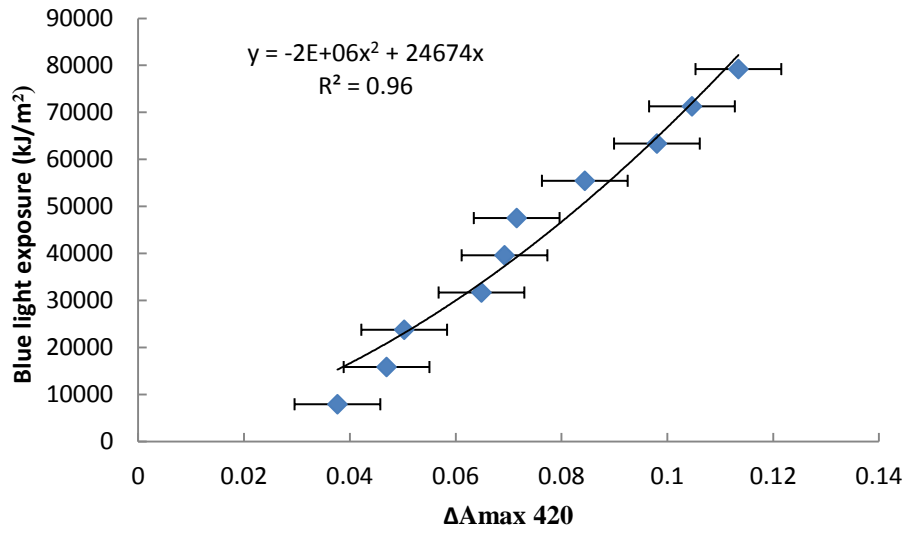


Figure 18 The dose response curve for the fluorescent tube light.

4.1.3 Influence of the Angle of the Receiving Plane

Figure 19 shows the contrast of cosine response of the blue light dosimeter to the cosine curve. The influence of the angle of the receiving plane of the blue light hazard dosimeter (VIS_{BL}) compared with the cosine function for angles from 10° to 70° and the error bars describe the average for post exposure absorbance measurements.

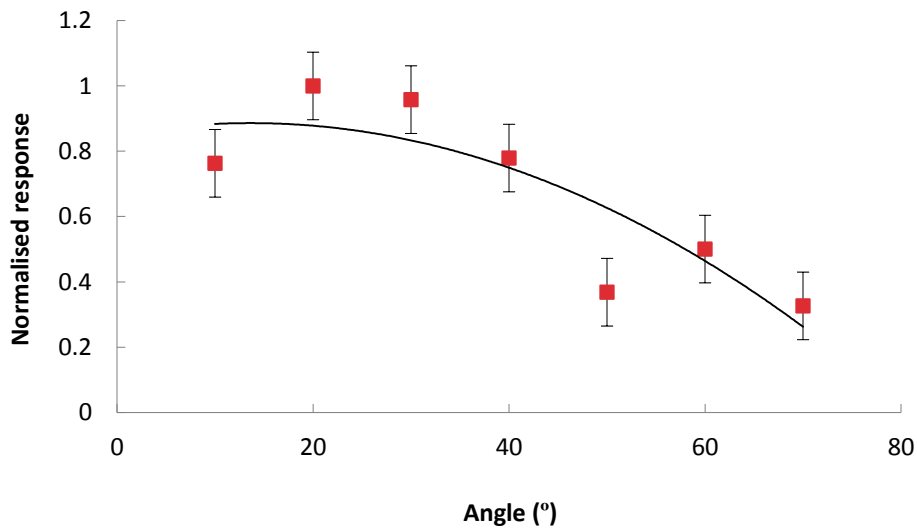


Figure 19 The response to a collimated beam incident at a plane inclined for the following angles: 10° , 20° , 30° , 40° , 50° , 60° and 70°

4.1.4 Dose Rate Independence

Figure 20 shows the change in absorbance for the same total exposure at different irradiances. It also illustrates the relationship between the change in absorbance and the blue light irradiance; the y-axis error bars represent the standard deviation in ΔA of the absorbance data due to the irradiance. There was no significant change for irradiances between 5 W/m² and 7 W/m². The response of the dosimeters for blue light irradiance showed a small increasing trend from 10 W/m² to 15 W/m², however the averages are still within the error bars of those for the lower irradiances.

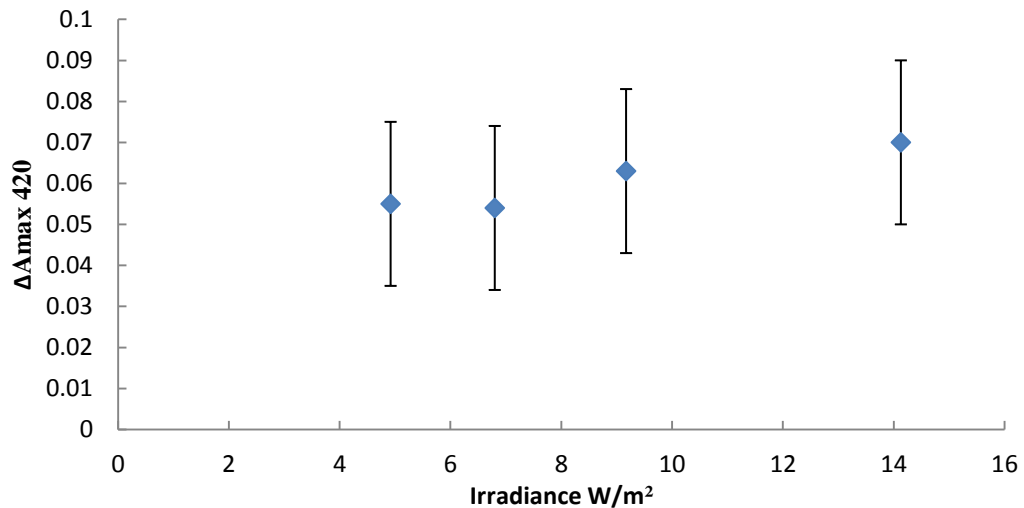


Figure 20 The change in absorbance at different irradiances at different distances of 5 cm, 10 cm, 15 cm and 20 cm

4.1.5 Dark Reaction

The dark reaction of both polysulphone and phenothiazine films is shown in Table 10 for the change in absorbance after periods of zero hour, one day and seven days after exposure.

Table 10 Dark reaction (zero hours, one day and seven days)

Time after exposure	0 hours	1 day	7 days
Average	0.056	0.058	0.067
Standard Deviation	0.041	0.048	0.049

The dark reaction of the blue light dosimeter was measured at 420 nm for different periods of zero hour, one day and seven days after exposure. Figure 19 shows the $\Delta A_{\text{MAX}} 420$ at each point.

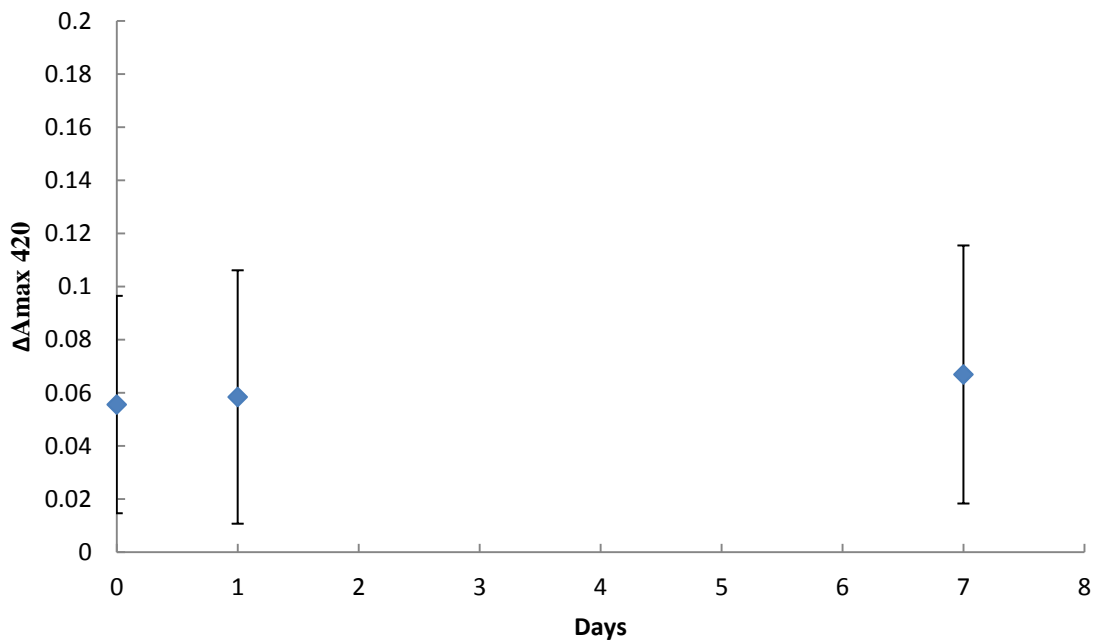


Figure 21 The dark reaction of the blue light dosimeters at periods of zero hours, one day and seven days

4.1.5.1 Reproducibility

For the reproducibility tests, fifteen dosimeters were exposed to the sun light over one day. The results show that the average in the change in absorbance was 0.056 with a standard error of 0.005.

4.1.6 Temperature Independence

Figure 22 shows the change in absorbance calculated for the blue light hazard dosimeters exposed at different temperatures for four different time periods and between 23 °C and 37 °C no response was found between the temperature and the response.

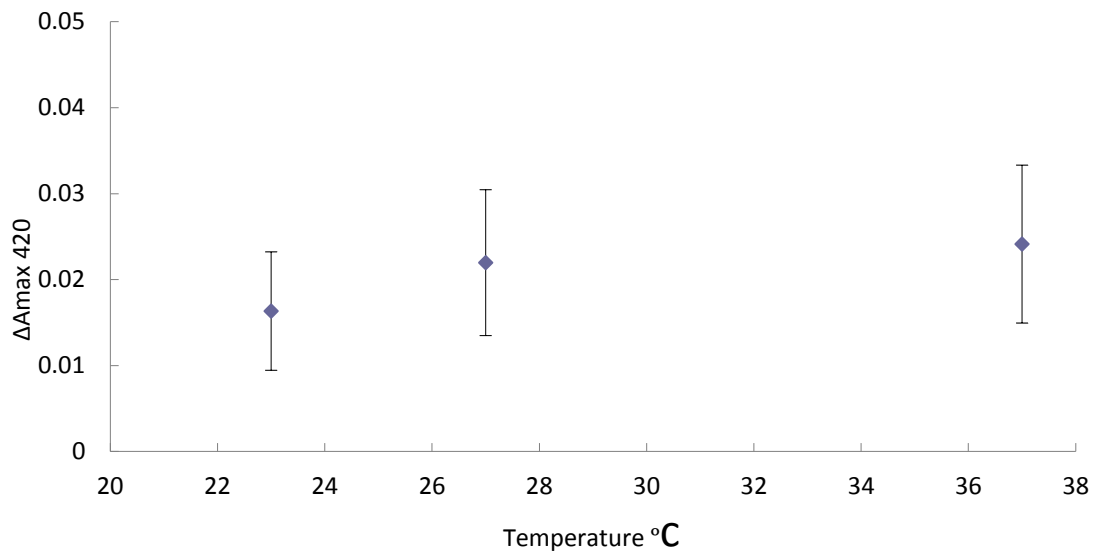


Figure 22 The change in absorbance for temperatures between 20° and 40° with the average for each dosimeter

5. CHAPTER FIVE

5.1 Discussion

5.1.1 Change in Absorbance

The spectral transmission of the blue light dosimeter was measured pre exposure and post exposure from 300 nm to 600 nm in a spectrophotometer to both sun light and a compact fluorescent lamp. As can be seen from Figures 13 and 14, from 300 nm to 600 nm, the maximum change in optical transmission after an exposure was approximately at 420 nm. Consequently, 420 nm was chosen as wavelength to determine the calibration of the VIS_{BL} dosimeter. That was comparable to the maximum change in optical transmission previously found at about 437 nm (Turnbull and Parisi, 2012).

5.1.2 Dose Response

All dose response calibration curves were calculated by exposing the films on a horizontal plane using three films of polysulphone, phenothiazine and Llumiar to make the dosimeter. The dosimeters for the dose response were exposed to different sources of light including the solar simulator, a fluorescent tube, a compact fluorescent light and a LED light. Each source had different exposure periods to calculate the change in absorbance and determine the dose response.

First, dosimeters were exposed to a LED light for different periods to determine the required exposure times. As can be seen in Figure 15, there is a change in the absorbance

of the dosimeters due to the LED light. Also, the change in absorbance shows increasing response with increasing exposure of the dosimeters from 0.04 to 0.07.

The second type of light source was a compact fluorescent light. The dosimeters were exposed to this light at 10 cm during ten days to provide a dose response. As shown in Figure 16, there is a response of the dosimeter to the light from the compact fluorescent lamp. However, there is a reasonable scatter of the values. Also, there is not much increasing response between the change in absorbance and the blue light exposure. This may be due to the need to have a more uniform coverage of the dosimeters by this compact fluorescent light.

The third type of light source was a solar simulator to provide a dose response. For eight times, at each half hour interval the dosimeter was measured for the post exposure absorbance to determine the dose response. Figure 17 shows the relationship between the change in absorbance and the blue light exposure through an equation that goes through the origin to describe the relationship. The error bars illustrate the standard deviation for each point.

The last light source for the dose response was a fluorescent tube. The period of exposure for the dosimeters was ten days to measure the dose response calibration curve. Figure 18 shows that the change in absorbance is increasing from 0.03 to 0.12. In summary, the blue light hazard dosimeters have been measured for their dose response to diverse periods for different light sources on a horizontal plane.

5.1.3 Influence of the Angle of the Receiving Plane

The dosimeter was tested for the cosine response with a solar simulator. This dosimeter was exposed at different angles from the normal plane to the incident irradiance from 10° to 70° degrees. As can be seen from Figure 19, the error bars are the standard deviation of the statistics for all points. The change in absorbance of the dosimeter at a given angle was normalized so that it could be compared with the cosine curve. The normalized response of the dosimeter was predominantly within the error bars of the cosine curve for the range up to 70° . The variation between the influence of the angle of the receiving plane of the dosimeter and the theoretical response was approximately 0.2 or less. In comparison, Jia et al. (2010) found the difference between the cosine response of the dosimeter and the theoretical response was less than 0.1.

5.1.4 Dose Rate Independence

The dose rate independence of blue light irradiance refers to the rate of change of the absorbance of the dosimeter. For dose rate independence tests, the dosimeters were exposed to the fluorescent tube for a range of times at different distances of 5 cm, 10 cm, 15 cm and 20 cm during four days. As indicated in Figure 20, the VIS_{BL} dosimeter has a consistent ΔA for the irradiance range within which it will be used of 5 W/m² and 7 W/m². The observed change in response between 10 W/m² and 15 W/m² is within the error of measurement of the dosimeters ($\pm 10\%$).

5.1.5 Dark reaction

Dark reaction showed the change in absorbance for the three different time periods measured. The dosimeter was returned to the light free environment and removed to be measured again after 24 hours following the initial removal from the irradiance and finally measured again after seven days. Table 10 shows that the average change in absorbance was from 0.056 to 0.058 after twenty four hours with an increase to 0.067 after a week. In comparison the dark reaction had the average change in absorbance of -7.0 % and -11.3 % after 24 hours and 1 week, respectively (Turnbull & Parisi, 2012). Also, Davis et al. (1976) found that polysulphone had a dark reaction of 4% after 24 hours and 5% after one week. Consequently, the dark reaction was taken into account during the field use of the dosimeter by measuring the post exposure absorbance of the VIS_{BL} dosimeters after a consistent time period following exposure.

5.1.5.1 Reproducibility

For the reproducibility tests, dosimeters were situated on a horizontal plane and exposed to the sun light for four hours. The reproducibility test found the dosimeters exposed to the same exposure of solar radiation provided a standard error in the change in absorbance of 0.005. This is comparable to the standard deviation for polysulphone of 11% (Turnbull & Parisi 2012).

5.1.6 Temperature Independence

The temperature independence was established by recording the change in absorbance of the dosimeter at different temperatures. It was tested at temperatures between 20° and 40° C exposed on a horizontal plane to the fluorescent lamp. As indicated in Figure 22, the temperature independence was found as the dosimeters response did not change with temperature from 23 °C to 37 °C. The change in absorbance of the dosimeter was within the error bars of the ΔA from 23 °C to 37 °C. These results indicate that the dosimeter was independent of the temperature over the range of 23 °C to 37 °C.

5.2 Significance

Blue light can be damaging to the human eye. In order to reduce the implications on public health due to the blue light hazard, it is necessary to first quantify the amount of blue light received by humans during normal daily activities. A potential dosimeter for measuring the blue light hazard effective wavelengths has been proposed (Turnbull and Parisi, 2012). This current project has extended this previous research to characterise the properties of this dosimeter for quantifying the blue light hazard exposures.

5.3 Future Directions

Future research using a blue light hazard dosimeter based on polysulphone and phenothiazine could measure different exposures of blue light and UV radiation including in different seasons and environments and to the human body and plants. Future directions with these dosimeters include:

- Investigate how to extend the dynamic range of the dosimeter to more than one day for use in sunlight.
- Examine the dose response of the polysulphone and phenothiazine dosimeters over a range of angles; this would determine if the calibration that is done on a horizontal plane is valid for exposures at a range of angles.
- Investigate if a combined dosimeter of polysulphone with phenothiazine is useful in determining the blue light hazard exposures to humans during normal activities.
- Measure the dose response from a stronger LED light would be useful to determine the dose response in future research.

- Measure the dose response from a higher intensity of a compact fluorescent light source.
- Determine the appropriate corrections to be made for temperature independence in further studies.
- Further research needs to be undertaken on the saturation of these dosimeters.

6. CHAPTER SIX

6.1 Conclusion

Exposure to blue light can be harmful to the human eye, especially the retina. Blue light has been established to cause a reaction in the eye and has been characterized by the International Commission on Non- Ionising Radiation Safeguard as the blue light hazard. Different dosimeters have been used to measure the blue light exposure lasting longer than one day including one made from polysulphone, phenothiazine and Llumar films. This study aimed to establish whether this proposed blue light dosimeter has the properties suitable for measuring ocular blue light hazard exposures.

The objective was to confirm that useful dosimetry based on polysulphone and phenothiazine can measure the blue light hazard exposure. This was done by quantifying the characteristics of the dosimeter including: change in absorbance, dose response, influence of the angle of the receiving plane, dark reaction, reproducibility, dose rate independence and temperature independence.

The change in the optical transmission due to blue light exposure was found. The response of the dosimeter indicated a maximum change due to the exposure at approximately 420 nm. The polysulphone and phenothiazine dosimeters were exposed to four light sources and a dose response calibration curve between the blue light exposure and the change in absorbance was established. The influence of the angle of the receiving plane was found to be similar to the ideal cosine function for angles up to 70° from the normal.

The variation between the influence of the angle of the receiving plane of the dosimeter and the ideal response was less than 0.2. The reproducibility of the dosimeters for the same exposures of solar radiation showed a maximum in the standard error of the change in absorbance of 0.005. The dark reaction had been found and the average of the change in absorbance was 0.056 after zero hours and 0.058 after twenty four hours and 0.067 after a week.

The dose rate independence showed that the response of the dosimeters does not depend on the different distances or irradiances. This is for the irradiance range 5 W/m² to 7 W/m². The observed change in response between 10 W/m² and 15 W/m² is within the error of measurement of the badge ($\pm 10\%$). The temperature tests found that the dosimeters do not respond to temperature from 23 °C to 37 °C.

This research has concluded that the polysulphone and phenothiazine film dosimeter has the suitable properties to allow it to be used in research to measure the blue light hazard exposure.

7. REFERENCES

- CIE (International Commission on Illumination) 1987, 'A reference action spectrum for ultraviolet induced erythema in human skin', *CIE J.* vol. 6, pp. 17-22.
- Davis, A., Deane, G.H.W. & Diffey, B.L. (1976), 'Possible dosimeter for ultraviolet radiation', *Nature*, vol. 261, pp. 169-170.
- Diffey, B. L. (2002), 'Sources and measurement of ultraviolet radiation', *Methods*, vol. 28, no.1, pp. 4-13.
- Diffey, B.L. (1984), 'Personal ultraviolet radiation dosimetry with polysulphone film badges', *Photodermatol*, vol. 1, pp. 151-157.
- Fletcher, A., Bentham, G., Agnew, M., Young, I., Augood, C., Charkravarthy, U., de Jong, P., Rahu, M., Seland, J., Soubrance, G., Tomazzoli, L., Topouzis, F., Vingerling, J. & Vioque, J. (2008), 'Sunlight exposure, antioxidants, and age-related macular degeneration', *Arch Ophthalmol*, vol. 126, no. 10, pp. 1396-1403.
- Forgan, B. & McGlynn, P. (2010), 'Developing UV monitoring with CCD technology', *NIWA Information Series*, no. 77, pp. 11-12.
- Gies, P., & Roy, C. R. (1988), 'Ocular protection from ultraviolet radiation', *Clinical and Experimental Optometry*, vol. 71, no. 1, pp. 21-27.
- "Health Effects of Artificial Light", Scientific Committee on Emerging and Newly Identified Health Risks- SCENIHR 2012.
- ICNIRP (International Commission on Non-Ionising Radiation Protection) (1997), 'Guidelines on limits of exposure to broad-band incoherent optical radiation (0.38 to 3 μm)', *Health Physics Society*, vol. 73, no. 3, pp. 539-554.
- Jia, K., Parisi, A. V., & Kimlin, M. G. (2010), 'Phenothiazine UVA dosimeter: characteristics and performance', *Photochemical & Photobiological Sciences*, vol. 9, no. 9, pp. 1224-1227.
- Kazadzis, S., Bais, A., Kouremeti, N., Gerasopoulos, E., Garane, K., Blumthaler, M., Schallhart, B. & Cede, A. (2005), 'Direct spectral measurements with a Brewer spectroradiometer: absolute calibration and aerosol optical depth retrieval', *Applied Optics*, vol. 44, no. 9, pp. 1681-1689.
- Okuno, T., Ojima, J. & Saito, H. (2010), 'Blue-light hazard from CO₂ arc welding of mild steel', *Annals of Occupational Hygiene*, vol. 54, no. 3, pp. 293-298.

- Oliva, M. S., & Taylor, H. (2005), 'Ultraviolet radiation and the eye', *International Ophthalmology Clinics*, vol. 45, no. 1, pp. 1-17.
- Parisi, A. V., Kimlin, M. G., Turnbull, D. J., & Macaranas, J. (2005), 'Potential of phenothiazine as a thin film dosimeter for UVA exposures', *Photochem. Photobiol. Sci.*, vol. 4, no. 11, pp. 907-910.
- Parisi, A. V., Sabburg, J., & Kimlin, M. G. (2004), '*Scattered and filtered solar UV measurements*', vol. 17, Kluwer Academic Publishers, Dordrecht.
- Roberts, D. (2011), 'Artificial lighting and the blue light hazard', *Macular Degeneration Support*, pp. 1-20.
- Rosenthal, F., Safran, M. & Taylor, H. (1985), 'The ocular doses of ultraviolet radiation from sunlight exposure', *Photochemistry and Photobiology*, vol. 42, no. 2, pp. 163-171.
- Roy, C.R., Gies, H.P. & Toomey, S. (1995), 'The solar UV radiation environment: measurement techniques and results', *Journal of Photochemistry and Photobiology B: Biology*, vol. 31, pp. 21-27.
- SCENIHR (2012), 'Health effects of artificial light,' Scientific Committee on Emerging and Newly Identified Health Risks.
- Sliney, D. H. (2001), 'Photoprotection of the eye—UV radiation and sunglasses', *Journal of Photochemistry and Photobiology B: Biology*, vol. 64, no. 2, pp. 166-175.
- Sliney D.H. (2012), 'How light reaches the eye and its components', *Int J Toxicol 2002; 21: 501-9 and Health Effects of Artificial Light*, SCENIHR.
- Smith, B., Belani, S. & Ho, A. (2005), 'Ultraviolet and near-blue light effects on the eye', *International Ophthalmology Clinics*, vol. 45, no. 1, pp. 107-115.
- Taylor, H. (1989), 'Ultraviolet radiation and the eye: An epidemiologic study', *From the Dana Center for Preventive Ophthalmology*, pp. 802-853.
- Turnbull, D. J., & Parisi, A. V. (2012), 'Potential dosimeter for quantifying biologically effective blue light exposures', *Radiation Protection Dosimetry*, vol. 149, no. 3, pp. 245-250.
- van Norren, D., & Gorgels, T. G. M. F. (2011), 'The action spectrum of photochemical damage to the retina: a review of monochromatic threshold data', *Photochemistry and Photobiology*, vol. 87, no. 4, pp. 747-753.
- Walker, D., Vollmer-Snarr, H. & Eberting, C. (2012), 'Ocular hazards of blue-light therapy in dermatology', *J Am Acad Dermatol*, no. 66, pp. 130-5.

Wengraitis, S., Benedetta, D. & Sliney, D. (1998), 'Intercomparison of effective erythral irradiance measurements from two types of broad-band instruments during 1995', *Photochemistry and Photobiology*, vol. 68, no. 2, pp. 179-182.

Young, R. W. (1994), 'The family of sunlight-related eye diseases', *Optometry & Vision Science*, vol. 71, no. 2, pp. 125-144.

8. LIST OF ABBREVIATIONS

AMD Age macular degeneration

UV Ultraviolet

UVA Ultraviolet A (320 - 400 nm)

UVB Ultraviolet B (280 – 320 nm)

PS Polysulphone

NDA Nalidixic acid

ΔA Change in absorbance

RPE Retinal pigmented epithelium

ICNIRP International Commission on Non- Ionizing Radiation
Protection

IL International Light

VIS_{BL} Blue light hazard dosimeter

$\lambda_{\Delta A_{max}}$ Wavelength at the maximum change in absorbance

